

# Cascades in nonlocal turbulence

Gregory Falkovich<sup>1,2</sup> and Natalia Vladimirova<sup>3</sup>

<sup>1</sup>*Weizmann Institute of Science, Rehovot 76100 Israel*

<sup>2</sup>*Institute for Information Transmission Problems, Moscow, 127994 Russia*

<sup>3</sup>*University of New Mexico, Department of Mathematics and Statistics, Albuquerque NM 87131*

(Dated: October 2, 2018)

We consider developed turbulence in the 2D Gross-Pitaevsky model, which describes wide classes of phenomena from atomic and optical physics to condensed matter, fluids and plasma. The well-known difficulty of the problem is that the hypothetical local spectra of both inverse and direct cascades in the weak-turbulence approximation carry fluxes which are either zero or have the wrong sign; such spectra cannot be realized. We analytically derive the exact flux constancy laws (analogs of Kolmogorov's 4/5-law for incompressible fluid turbulence), expressed via the fourth-order moment and valid for any nonlinearity. We confirm the flux laws in direct numerical simulations. We show that a constant flux is realized by non-local wave interaction in both the direct and inverse cascades. Wave spectra (second-order moments) are close to slightly (logarithmically) distorted thermal equilibrium in both cascades.

Turbulence is a state where pumping and dissipation happen at very different scales, so that the main issue is the nature of the transfer of a conserved quantity (say, energy) from pumping to damping due to nonlinear interaction. Despite the fundamental importance of this process, there is a certain terminological (and even conceptual) confusion surrounding the notion of locality of turbulence cascades. It may seem clear intuitively: either the energy is transferred locally in  $k$ -space by a cascade-like process or jumps directly from the motions of pumping scales to those of damping scales.

The problems start when one tries to formally sort out how locality or non-locality is manifested in the correlation functions. The simplest case is that of a complete scale invariance when the statistics at the scales between the pumping scale  $l_p$  and the damping scale  $l_d$  are independent of  $l_p$  and  $l_d$ ; it is then natural to call it a local cascade. Such cases do exist at least for some inverse cascades; however, scale invariance is spontaneously broken in direct cascades, see e.g. [1]. Indeed, the direct energy cascade in 3D has  $l_p$  explicitly entering all the velocity structure functions except the third, which determines the energy flux through the scale  $r$ . The same is true for the direct vorticity cascade, where all velocity and vorticity correlation functions contain  $l_p$ , again, except the triple moment expressing the flux of squared vorticity [2–4]. Are we to call such turbulence non-local, because the pumping scale explicitly determines the moments (including the second one, i.e. the energy spectrum), or to classify it as a local cascade, because the flux through the scales is constant?

One finds even more confusion in weak turbulence theory, which aspires to provide a close description solely in terms of the second moment – if it contains  $l_p$  and/or  $l_d$ , turbulence is called non-local [5]. We wish to state here that even in such cases there must exist a higher-order correlation function which is universal, i.e., dependent neither on  $l_p$ ,  $l_d$  nor on mechanisms of pumping and dissipation.

It is thus important to clearly distinguish non-locality

of turbulence (when some correlation functions in the inertial interval depend on the pumping and/or dissipation scales) and locality of the flux, which corresponds to a single correlation function independent of  $l_p$  and  $l_d$ . Locality of the flux is, in a sense, a trivial consequence of a conservation law, and it may co-exist with the non-locality of turbulence.

Here we show that such co-existence takes place for 2D turbulence in the framework of the Gross-Pitaevsky model. We derive universal (i.e., independent of  $l_p$ ,  $l_d$ ) flux relations for both direct and inverse cascades. These universal flux relations are expressed via the fourth moments. And yet we show that both cascades are not scale-invariant, so that the second moments (and spectral densities) explicitly depend on the pumping and dissipation scales.

The Gross-Pitaevsky model is one of the most universal models in physics. It describes wave propagation in wide classes of phenomena in fluids, solids and plasma. Applications include light propagating in media with the Kerr nonlinearity [6], and non-equilibrium states of cold atoms in Bose-Einstein condensates [7].

The range of applications is broad because the physical model is built on a single assumption: the narrow distribution in the space of momenta of wave vectors. The complex wave envelope,  $\psi$ , then evolves according to the Gross-Pitaevsky, or nonlinear Schrödinger equation,

$$\psi_t = i\nabla^2\psi + is|\psi|^2\psi. \quad (1)$$

On the right-hand side, the first term describes a linear propagation, and the second term represents nonlinear interaction (of waves or particles). The parameter  $s$  in front of the nonlinear term distinguishes the focusing/attractive ( $s = +1$ ) and defocusing/repulsive ( $s = -1$ ) cases.

Equation (1) has two integrals of motion (conserved quantities): the wave action,  $\mathcal{N} = \int |\psi|^2 d\mathbf{r}$ , and the Hamiltonian,  $\mathcal{H} = \int |\nabla\psi|^2 - \frac{1}{4}s|\psi|^4 d\mathbf{r}$ . Assuming a weak nonlinearity, it can be shown that the cascade of wave action in spectral space is inverse [5], i.e., directed to-

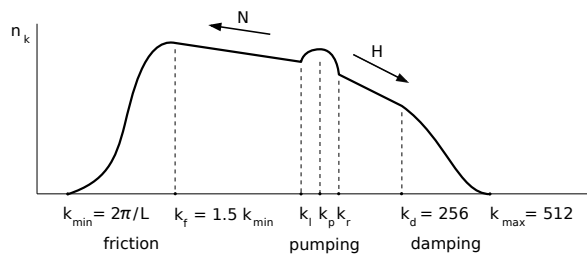


FIG. 1: Schematic representation of forcing and damping in spectral space.

ward small wave numbers, while the cascade of the energy is direct. Independent of the sign of the nonlinearity, the inverse cascade results in the appearance of large, spatially-coherent structures [8, 9], and, in the case of the defocusing nonlinearity, in the accumulation of condensate — the mode that is spatially-coherent across the whole system. In this study, however, we avoid condensate creation by adding dissipation at low  $k$ . Therefore, even though we work with  $s = -1$ , some of our results could be relevant to the focusing case as well.

We numerically solve Eq. (1) with the defocusing nonlinearity, using a standard split-step method [8] modified to be 4th-order accurate in time. Forcing and damping, applied in spectral space, are represented in the r.h.s. of the equation,

$$i\psi_t + \nabla^2\psi - |\psi|^2\psi = i\hat{f}_k\psi + i\hat{g}_k. \quad (2)$$

We use the same code as in [10], with the numerical method described in detail in [11]. Our computational domain is square,  $L \times L$ , with periodic boundary conditions, so that the lowest wave number is determined by the domain size,  $k_{\min} = 2\pi/L$ . All simulation presented here are done at the same resolution,  $\Delta x = \Delta y = 2\pi/1024$ , and time step  $\Delta t \leq 10^{-5}$ . We use domains up to  $L = 32\pi$ , with grids up to  $16386^2$  points.

To deposit wave action into the system we use the additive forcing,  $g_k = |g_k|e^{i\phi_k}$ , with random phases  $\phi_k$  and amplitudes  $|g_k| \propto \sqrt{(k^2 - k_l^2)(k_r^2 - k^2)}$  which are non-zero only in a ring of wavenumbers  $k \in [k_l, k_r]$ . The forcing is normalized to deposit a specified amount of wave action,  $\dot{N} \equiv \alpha$ , where  $N = \langle |\psi|^2 \rangle$  and angular brackets denote spatial averaging. The multiplicative forcing,  $f_k = -\beta(k/k_d)^4(k/k_d - 1)^2$ , provides small scale damping at  $k > k_d$ . We use  $k_d \approx 3k_r$  to include a contribution of cubic nonlinearity to the direct cascade. In addition to high- $k$  damping, we have an option to include low- $k$  friction,  $f_k = -(1, 1, \frac{1}{\sqrt{2}})\gamma$  for  $k = (0, 1, \sqrt{2})k_{\min}$ . Unless otherwise specified, we use  $\gamma = 6.2\alpha^{\frac{2}{3}}$ . To distinguish dissipation at low and high wavenumbers we will refer to them respectively as “friction” and “damping” to stress that they play different roles. The purpose of friction is to absorb the wave action and prevent the accumulation of condensate, while the purpose of damping is to absorb

the energy and limit the spectrum to a finite number of modes.

One advantage of running at the same resolution is that we can use the same damping parameters,  $k_d = 256$  and  $\beta = 400$ , in all simulations. Our studies of the inverse cascade are done with pumping rings with  $k_l = 68$  and  $k_r = 84$ , while our simulations of the direct cascade are done with  $k_l = 6k_{\min}$  and  $k_r = 9k_{\min}$ . The strength of forcing and friction are controlled by  $\alpha$  and  $\gamma$  respectively, which are treated as simulation parameters.

Notice that  $\alpha$  is an input rate of wave action into the system, which is close to but not exactly equal to the flux into the inverse cascade,  $\tilde{\alpha}$ . In our simulations of the inverse cascade, at most 10% of wave action is lost to damping, that is  $\tilde{\alpha} \gtrsim 0.9\alpha$ . The lost fraction is measured by computing the wave action consumed by friction in a steady state, and also from simulations without friction, where the slope of  $N(t)$  initially matches the rate of wave deposition  $\alpha$  and switches to  $\tilde{\alpha}$  later.

We start with the demonstration that the flux laws expressed in terms of fourth moments are exact and local, that is, independent of  $k_p$  and  $L$ . Let us consider steady-state turbulence and look at the following quantity,  $\langle |\psi_1 - \psi_2|^2 \rangle$ . Here,  $\psi_1$  and  $\psi_2$  refer to the values at two points separated by the distance  $r$  taken in the interval of the inverse cascade,  $L \gg r \gg k_p^{-1}$ . This second moment can be related to the spectral density:

$$\langle |\psi_1 - \psi_2|^2 \rangle = \int |\psi_k|^2 (1 - \cos kr) dk \simeq \int_{1/r}^{\infty} |\psi_k|^2 dk.$$

Next, we use Eq. (2) to take the time derivative of

$$\langle |\psi_1 - \psi_2|^2 \rangle = 2N - \langle \psi_1\psi_2^* + \psi_1^*\psi_2 \rangle$$

and obtain,

$$Q(r) \equiv 2\text{Im}\langle \psi_1^*\psi_2^2\psi_2 \rangle = -\tilde{\alpha}. \quad (3)$$

This exact flux relation is valid for any dimensionality. Note that the right hand side is an outcome of all mechanisms of pumping and dissipation acting at the scales smaller than  $r$ , i.e., the effective flux of the wave action into the inverse cascade. This result is non-trivial because it shows that the fourth correlation function  $Q(r)$  is the divergence of the wave action flux, which is equal to the input rate in the steady state, and thus does not depend on the distance  $r$ .

Simulations with different input rates show that  $Q(r)$  scales as  $\alpha$  in the range from the damping scale to the size of the domain, for both the direct and inverse cascades. Simulations of the inverse cascade confirm the appearance of the plateau,  $Q(r) = -\tilde{\alpha}$  for  $r \gtrsim r_p$ , as shown in Fig. 2, left panel. Here, we have filtered out small-scale oscillations  $r < r_p$ , resulting from spectrally narrow pumping.

For the direct energy cascade, one generally cannot obtain a scale-invariant flux law since the energy contains two terms: the quadratic kinetic term  $|\nabla\psi|^2$  and

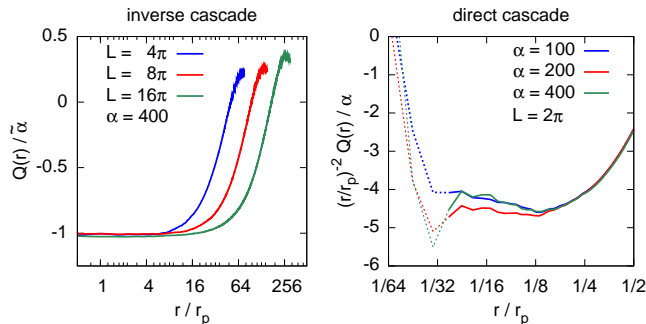


FIG. 2: The ratio of the correlation function  $Q(r)$  to the input rate of wave action in simulations of inverse and direct cascades (left and right panels respectively). The data are collected over time and averaged in angular direction. The filter removing harmonics with  $k > k_l$  is applied before averaging in the inverse cascade runs. Dashed lines are data in the damping interval of scales. (Color online.)

the quartic potential term  $|\psi|^4$ . At least for not very strong nonlinearities, when potential energy is not very large, we expect the kinetic energy flux,  $P = \nabla^2 Q$ , to be scale-independent, or equivalently  $Q(r) \sim r^2$ . The right panel of Fig. 2 shows that indeed  $Q(r)/\alpha \approx -4.5(r/r_p)^2$ , resulting in  $P \approx -18\alpha r_p^{-2}$ , for  $r \lesssim 0.2r_p$ .

Note that our simulations of systems evolving freely, without friction, show that there is no time interval when the flux  $Q$  is constant in the inverse cascade, while the region  $Q \propto r^2$  is formed in the direct cascade region. Thus, the flux law (3) is specific to steady spectra. This by itself is already a signature of non-locality — indeed, in incompressible turbulence, the 4/5 law of the direct cascade takes place even for decaying turbulence, while the 3/2 law of the inverse cascade takes place at a given scale when larger scales continue to evolve, see e.g., [12, 13].

Next, we look at the spectra, starting with the inverse cascade. As was observed in [8, 9, 14, 15], such spectra are close to thermal equilibrium,  $n_k = T/(k^2 + k_\mu^2)$ , where the temperature  $T$  and chemical potential  $\mu \equiv k_\mu^2$  are system dependent parameters. The transition to the equipartition region,  $k_\mu$ , is independent of the size of the domain, as shown in Fig. 3. When the range of  $k$  is limited, there is no equipartition region at all.

We characterize the degree of nonlinearity by the ratio of the mean potential energy of interaction to the kinetic energy:  $H_p/H_k = \langle |\psi|^4 \rangle / \langle |\nabla\psi|^2 \rangle$ . In simulations with smaller nonlinearities ( $100 \leq \alpha \leq 800$ ,  $0.07 < H_p/H_k < 0.15$ ) the spectra have the weak-turbulence scaling,  $n_k \propto \alpha^{1/3}$  [5], confirming dominance of resonant four-way interactions (see Fig. 4a). The higher- $k$  parts of compensated spectra (to the immediate left of pumping) have a well-defined slope, which can be described by a logarithmic correction. This part of the spectrum is relatively insensitive to friction. There is a pile-up at low  $k$ ;

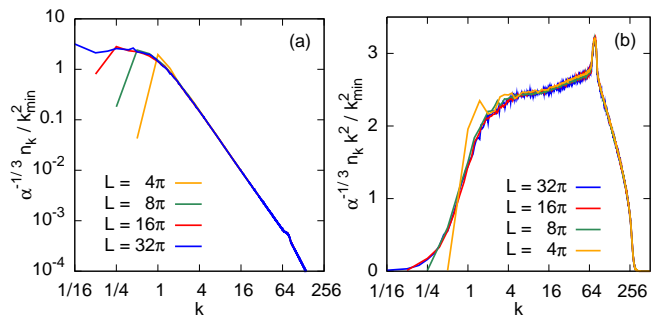


FIG. 3: Non-compensated (a) and compensated (b) spectra in simulations with different domain sizes with  $\alpha = 400$ . (Color online.)

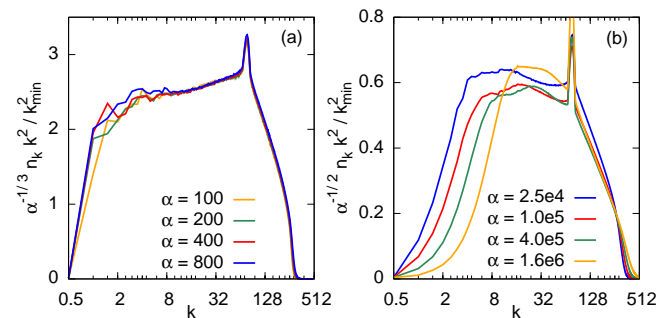


FIG. 4: Effect of pumping rate on stabilized spectra in simulations with  $L = 4\pi$ . At lower rates  $n_k \sim \alpha^{1/3}$  (a), while at higher rates  $n_k \sim \alpha^{1/2}$  and spectra develop equipartition region (b). Friction was selected to minimize the pile-up:  $\gamma = 6.2\alpha^{2/3}$  for  $\alpha \leq 800$  and  $\gamma = (250\alpha)^{1/2}$  for  $\alpha \geq 2.5 \times 10^4$ . (Color online.)

the amplitude and location of the pile-up depend on the friction. Adjusting  $\gamma$ , we can minimize the pile-up but cannot eliminate it completely.

The pile-up is more pronounced at higher nonlinearities ( $2.5 \times 10^4 \leq \alpha \leq 1.6 \times 10^6$ ,  $0.4 < H_p/H_k < 1.5$ ) eliminating the part of the spectrum that logarithmically decreases towards lower  $k$  (Fig. 4b). At high nonlinearities we start to observe a region with action equipartition. The gap at low  $k$  in Fig. 4b is similar to the gap in Fig. 3b; the higher  $\alpha$ , the wider the gap. Unlike the amplitude of the pile-up, which is very sensitive to friction, the width of the gap is relatively robust; the friction only slightly affects the width of the equipartition region.

At high input rates the overall level of spectra changes from  $n_k \propto \alpha^{1/3}$  scaling to  $n_k \propto \alpha^{1/2}$ , suggesting transition to three-way interactions, which are non-resonant without a condensate. It could well be that in our case the role of condensate (or “pre-condensate”) is played by the collection of low- $k$  modes. To analyze the degree of coherence between these modes and their role in interactions with the rest of the spectrum remains a subject for

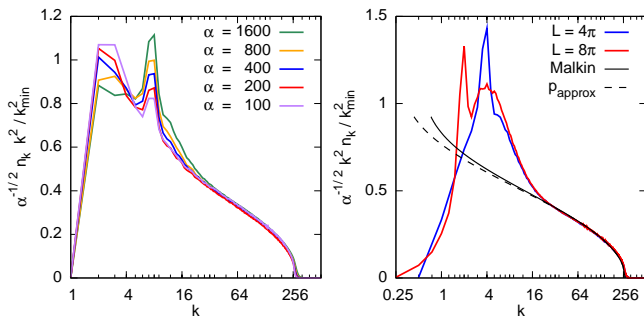


FIG. 5: Left: Spectra of direct cascade for  $L = 2\pi$  and different  $\alpha$ . Right: Spectra with  $\alpha = 400$  compared with Malkin model, fit with  $C = 88$ . (Color online.)

future work.

A pile-up and low- $k$  equipartition, similar to those shown in Figs. 3 and 4, was observed in simulations of water wave turbulence and attributed to the bottleneck [16] due to lack of low-frequency modes [21]. In our case, we can rule out this explanation, since our simulations performed in increasing domains show the appearance of the equipartition region even for moderate  $\alpha$ . Note briefly that the form of the spectrum deviation suggested in [8] is not supported by our data.

Next, we describe the steady-state spectra of the direct cascade, shown in Fig. 5. Far from the pumping, the spectra scale as  $n_k \propto \alpha^{1/2}$ , similarly to inverse cascades with high nonlinearities. As we extend our computational domain, we observe a non-universal region at low  $k$  and a universal region at high  $k$  (in our case,  $k > 16$ ). We compare the shape of the spectra in the universal region to the theory by Malkin [17]. The theory assumes non-local weakly-nonlinear interaction and describes the shape of direct cascade in terms of  $N_k/N$ , which is the fraction of wave action contained within a sphere of radius  $k$ . The spectrum,  $n_k$ , is described implicitly through the following equations,

$$\frac{n_k k^2}{k_{\min}^2} = \frac{C}{2\pi} \left[ \ln \frac{N}{N_k} \right]^{\frac{1}{3}}, \quad (4)$$

$$\frac{C}{N} \ln \frac{k_M}{k} = p\left(\frac{N_k}{N}\right), \quad (5)$$

where  $C$  is a constant related to the energy flux, and  $k_M$  is the cut-off mode. The function  $p(m)$  is an integral which can be expressed in terms of the lower incomplete gamma function,  $\mathcal{P}(a, x)$ , e.g., Eq. (6.5.1) in [18],

$$p(m) = \int_m^1 \ln^{-\frac{1}{3}} \frac{1}{y} dy = \Gamma\left(\frac{2}{3}\right) \mathcal{P}\left(\frac{2}{3}, \ln \frac{1}{m}\right). \quad (6)$$

To compare our data and the theory predictions, we extract  $N_k/N$  from numerical simulations and verify Eq.(4) and Eq.(5) individually. The comparison shows a good agreement in the range  $\ln(N/N_k) \in [10^{-3}, 0.3]$ , or for

$N_k/N \in [0.74, 0.999]$ . We stress that the data is fitted with the single parameter,  $C = 88$  for  $\alpha = 400$ . The total wave action,  $N = 405$ , is computed from the simulations. As for the cutoff mode, we use  $k_M = 270$ , which works better than the damping cutoff,  $k_d = 256$ . Taking into account that damping is a smooth function of  $k$ , non-zero at  $k \gtrsim k_d$ , we find this modification acceptable. Once we have determined parameter  $C$  in Eqs.(4)-(5), we can combine these equations to describe the shape of the spectrum in a parametric representation shown with solid curve in Fig. 5, right panel. To provide an explicit expression for  $n_k(k)$ , one can approximate Eq. (6) as  $p_{\text{approx}}(m) = \frac{3}{2}(1-m)^{\frac{2}{3}}$ , which gives

$$\frac{n_k k^2}{k_{\min}^2} = \frac{C}{2\pi} \ln^{\frac{1}{3}} \left[ 1 - \left( \frac{2C}{3N} \ln \frac{k_d}{k} \right)^{\frac{3}{2}} \right]. \quad (7)$$

In the range  $k \in [16, 256]$  where the original theory agrees with the data, the approximation works as well as the original parametric representation. The agreement of the final expression with the data might not be impressive on its own (for example,  $n_k k^2 \propto \ln^{\frac{1}{2}}(k_M/k)$  also provides a good fit), however the agreement of underlying arguments gives additional support to the theory.

Our results can be extended beyond the single value of  $\alpha$ , by taking into account  $n_k \propto \alpha^{\frac{1}{2}}$  scaling, which leads to  $C = c\alpha^{1/2}$  with  $c \approx 4.4$ . To connect  $C \propto (n_k)^{\frac{2}{3}}$  to the energy flux, we recall our earlier observation,  $P = \nabla^2 Q \propto \alpha$ , illustrated in Fig. 2, to conclude that  $C \propto P^{1/3}$ , as proposed by Malkin. Yet nonlinearity restricts the range of applicability of the theory to the high- $k$  part of the spectrum. We speculate that the deviation at small  $k$  can be reduced, and the range of applicability could be extended, if the comparison were done for smaller  $\alpha$ .

It is instructive to compare briefly the 2D case considered here with the 3D case treated within the weak turbulence limit in [19, 20]. The inverse cascade is local in 3D [5, 19], while the spectrum of the direct cascade contains a logarithmic factor  $\log^{-2/3}(kl_p)$  [20].

To conclude, we have derived and confirmed exact fourth-order flux relations for both direct and inverse cascades. We have found the second moments and the spectra to be nonlocal for both cascades. The inverse cascade is weakly turbulent at low pumping rates, while nonlinearity is found to be substantial for the direct cascade at any input rate and for the inverse cascade at high input rates.

We wish to stress the general lesson: an exact flux relation, which contains neither pumping nor damping scale, must exist in the inertial interval of every turbulence. Such relation does not preclude turbulence from being non-local, as is the case for the direct cascade in 2D Navier-Stokes turbulence [4], and as is shown here for both cascades in 2D Gross-Pitaevsky model.

A part of this work was done during a visit to the Kavli Institute for Theoretical Physics, UCSB, supported by grant no. NSF PHY11-25915. N.V. was in part

supported by NSF grant no. DMS-1412140. Simulations were performed at the Center for Advanced Research Computing (CARC), UNM, and the Texas Advanced Computing Center (TACC) using the Extreme Science and Engineering Discovery Environment (XSEDE), which is supported by NSF grant no. ACI-

1053575. G.F.'s work is supported by grants of the Bi-National Science Foundation, Minerva Foundation with funding from the German Ministry for Education and Research and by Russian Science Foundation projects 14-22-00259 and 14-50-00150 (for the development of the analytical theory and writing the paper).

- 
- [1] G. Falkovich, *J Phys A: Math Theory* **42**, 123001 (2009).  
 [2] R. H. Kraichnan, *Physical Review Letters* **18**, 202 (1967).  
 [3] R. H. Kraichnan, *Physics of Fluids (1958-1988)* **10**, 1417 (1967).  
 [4] G. Falkovich and V. Lebedev, *Physical Review E* **50**, 3883 (1994).  
 [5] V. E. Zakharov, V. S. Lvov, and G. Falkovich, *Kolmogorov Spectra of Turbulence I: Wave turbulence* (Springer-Verlag, New York, 1992).  
 [6] C. Sulem and P. L. Sulem, *Nonlinear Schrödinger Equations: Self-Focusing and Wave Collapse* (World Scientific, New York, 1999).  
 [7] L. P. Pitaevskii and S. Stringari, *Bose-Einstein Condensation* (Clarendon, Oxford, 2003).  
 [8] S. Dyachenko, A. C. Newell, A. Pushkarev, and V. E. Zakharov, *Physica D* **57**, 96 (1992).  
 [9] A. Dyachenko and G. Falkovich, *Phys. Rev. E* **54**, 5095 (1996).  
 [10] N. Vladimirova, S. Derevyanko, and G. Falkovich, *Physical Review E* **85**, 010101 (2012).  
 [11] N. Vladimirova, S. Derevyanko, and G. Falkovich, arXiv preprint arXiv:1108.1541 (2011).  
 [12] U. Frisch, *Turbulence. The Legacy of A. N. Kolmogorov* (Cambridge University Press, Cambridge, 1995).  
 [13] G. Falkovich and K. Gawdzki, *Journal of Statistical Physics* **156**, 10 (2014).  
 [14] S. Nazarenko and M. Onorato, *Physica D: Nonlinear Phenomena* **219**, 1 (2006), ISSN 0167-2789.  
 [15] C. Sun, S. Jia, C. Barsi, S. Rica, A. Picozzi, and J. W. Fleischer, *Nature Physics* **8**, 470 (2012).  
 [16] G. Falkovich, *Physics of Fluids* **6**, 1411 (1994).  
 [17] V. M. Malkin, *Physical review letters* **76**, 4524 (1996).  
 [18] M. Abramowitz and I. A. Stegun, *Handbook of mathematical functions: with formulas, graphs, and mathematical tables*, 55 (Courier Dover Publications, 1972).  
 [19] V. Zakharov, *Sov Phys JETP* **35**, 908 (1972).  
 [20] G. Falkovich and I. Ryzhenkova, *Phys. Fluids B* **4**, 594 (1992).  
 [21] A. Korotkevich, private communications